

OBSERVATION OF MICROBUNCHING INSTABILITIES USING THz DETECTOR AT NSLS-II*

W. Cheng[#], B. Bacha, G. L. Carr

NSLS-II, Brookhaven National Laboratory, Upton, NY 11973

Abstract

Microbunching instabilities have been observed in several light sources with high single bunch current stored. The instability is typically associated with threshold beam currents. Energy spread and bunch length are increasing above the thresholds. Recently, a terahertz (THz) detector was installed at the cell 22 infrared (IR) beamline at NSLS-II storage ring to study the micro-bunch instabilities. The IR beamline has wide aperture allowing long-wavelength synchrotron radiation or microwave signal propagate to the end station, where the detector was installed. The detector output signal has been analyzed using oscilloscope, spectrum analyzer and FFT real-time spectrum analyzer. Clear sidebands appear as single bunch current increases and the sidebands tend to shift/jump. We present measurement results of the THz detector at different nominal bunch lengths and ID gaps.

INTRODUCTION

Microbunching instabilities have been observed at several storage rings [1-3], in earlier 2000. Bursts of coherent synchrotron radiation (CSR) in terahertz (THz) range were observed when beam current was above a certain threshold. Microstructure in the bunch, typically in the millimeter range (THz), is formed. The microstructure in the longitudinal phase space causes a sideband frequency component detectable with broadband THz detectors. More recent measurements [4-8] in low-alpha mode show stable CSR measured with broadband detectors. Schottky barrier diode (SBD) and quasi-optical detector (QoD) are easy to use with fast responses and high sensitivity.

NSLS-II storage ring has seen significant bunch lengthening and energy spread increases [9]. Earlier measurement of the beam spectrum shows higher order synchrotron motion sidebands appearance, indicating possible microstructure in the high current single bunch. To further understand the issue, a Quasi-optical detector (QoD) [10] has been prepared and setup at the visible diagnostic beamline and cell 22 infrared beamline (22-IR) at NSLS-II. The QoD has integrated broadband amplifier with 4GHz bandwidth. This allows bunch-to-bunch measurement with 2-ns bunch spacing. Recent observations from single bunch studies, as well as multi-bunch normal operations, are presented. It is worth to point out that most of the measurements were carried out with

normal lattice with momentum compaction factor of 3.63×10^{-4} . RMS bunch lengths are around 10-40ps, depending on the RF voltages, ID gaps and bunch lengthening.

EXPERIMENT SETUP

The 22-IR beamline at NSLS-II has been commissioned in 2018, collects bending magnet radiation from a large gap dipole in cell 23 (90mm magnet gap height, 76mm vacuum chamber inner height). The beamline is typically called 22-IR as it takes the experimental floor space facing cell 22 straight section. The beamline accepts synchrotron radiation fans of ~ 48 mrad horizontally. The vertical acceptance angle varies from 34-76 mrad along the dipole trajectory. The light is then guided through a series of Aluminum coated mirrors. The beamline layout is shown in Figure 1.

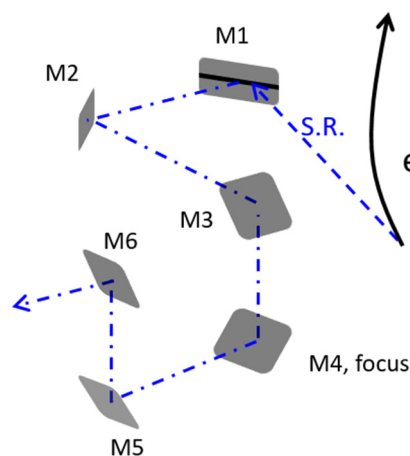


Figure 1: 22-IR beamline layout. Large gap dipole radiations are first reflected by the slotted first mirror (M1), then relayed to outside hutch through a series of mirrors. The concrete shielding wall is in-between M4/M5 mirrors.

The first mirror M1 locates at 2250mm from the dipole entrance. It has a wedge-shaped slot in the middle to let high power x-ray pass through. The slot has a vertical opening of 3mm at the location where electrons enter the dipole field, and increases linearly to about 6mm near the downstream edge. This is corresponding to open angle of 1.3 – 6 mrad for the slot. The wedge angle then increases so that the mirror profile matches the nominal vacuum chamber cross section (an octagon shape with 25mm high and 76mm wide). Long wavelength synchrotron radiations, including visible light, IR and far IR, are reflected by the M1 mirror and guided to the hutch on the experimental floor through other mirrors, as shown in Figure 1. M4 is a

*Work supported by DOE contract No: DE-SC0012704

[#]Weixing Cheng is now at Argonne National Laboratory, Email: wcheng@anl.gov

Content from this work may be used under the terms of the CC BY 3.0 licence (© 2019). Any distribution of this work must maintain attribution to the author(s), title of the work, publisher, and DOI

toroidal mirror which makes a 1:1 image, the other mirrors are all flat ones. Light passing through the concrete shielding wall in-between M4 and M5.

The QoD detector was installed in the 22-IR beamline hutch. A retractable reflection mirror was inserted after the M6 mirror which reflected the radiations outside the vacuum through a Pyrex viewport. The detector was mounted near the focal plane right on top of the viewport. QoD output signal was then fed to a spectrum analyzer or a high speed oscilloscope. Figure 2 shows the QoD setup in the 22-IR beamline hutch. The reflect mirror was inserted in the 4-way cross and reflected light upward through the viewport. A visible image spot was seen on the foil cutting from static shielding bag. The foil was used as density filter as there were too much signals for the QoD detector at high currents. The QoD was mounted ~1ft above the viewport, near the image plane.

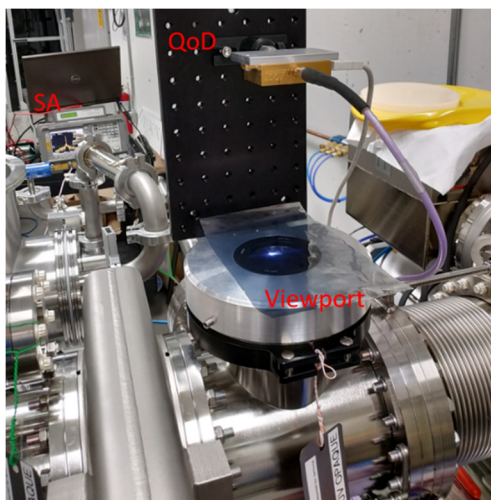


Figure 2: QoD setup in the IR beamline hutch.

Prior to the 22-IR beamline commissioning, the QoD detector had been setup at the visible diagnostic beamline. The beamline accepts 3mrad x 7mrad (horizontal x vertical) radiation fan. There were more than 10 meters of beam traveling in the air. Due to the smaller aperture and beamline configurations, QoD detects saw weaker signals compared to the IR beamline setup but still measurable.

MEASUREMENTS

With the QoD setup in the 22-IR beamline, various measurements have been carried out during studies or parasitic to user operations.

Single Bunch Spectrum

During a single bunch study shift, different single bunch currents were stored in the storage ring and QoD output spectra were measured on an FFT spectrum analyzer. Single bunch was first filled to high current (around 4-5mA), a horizontal scraper was then inserted to have the beam decay fast while QoD spectrum was recorded.

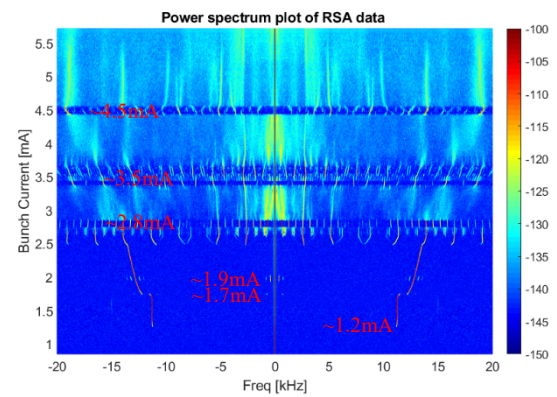


Figure 3: QoD signal spectra at different single bunch current. Vrf = 3MV, all ID gaps closed.

Figure 3 shows the spectrogram of QoD signal at various single bunch beam currents. In this case, all the insertion devices in the storage ring were closed, including 3 damping wigglers (DW), 6 elliptical polarized undulator (EPU) and 11 in-vacuum undulators (IVU). RF gap voltage was at 3MV contributed from two super-conducting RF cavities, with 1.5MV on each cavity. This is the typical configurations for the NSLS-II normal operation.

The FFT spectrum analyzer had center frequency at $5 \times \text{Fr}_f$ (~2.5GHz) and span of 40 kHz. The QoD spectrum was similar at other RF frequency harmonics.

As can be seen from the figure, the first sideband appeared at ~12kHz when single bunch current was above 1.2mA. The sideband shifted to higher frequency and jumped at 1.7mA. There was a small peak noticed at ~1kHz at the jump. With single bunch current continues increase, smaller sidebands were observed around the carrier frequency and main sideband at ~1.9mA. At 2.5mA, a lot more sidebands arose with three gaps at 2.8mA, 3.5mA and 4.5mA.

Changing ID gaps and RF voltages affect the sideband behavior. Figure 4-6 show the difference measured with 1) 3DW gaps closed, all other ID gaps open, RF voltage at 3MV; 2) All ID gaps open, RF voltage at 3MV; and 3) All ID gaps open, RF voltage at 1.5MV. In each case, the sideband appearing threshold currents were different and the behaviors varied differently as single bunch current increases. As the spectrum is symmetrical to the carrier frequency, only the upper side spectrum (0-20kHz) was plotted in these figures.

As the 0-current bunch lengths decrease (by changing the ID gaps and RF voltages), the threshold currents to see the first sidebands decreases. Table 1 summarizes the threshold current for the above situations.

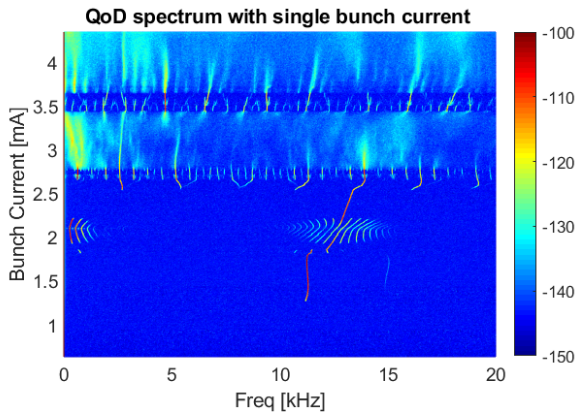


Figure 4: QoD signal spectra at different single bunch current. $V_{rf} = 3\text{MV}$, 3DW gaps closed, other ID gaps open.

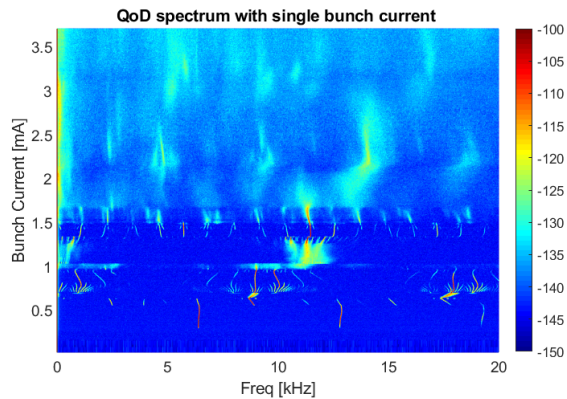


Figure 5: QoD signal spectra at different single bunch current. $V_{rf} = 3\text{MV}$, all ID gaps open (bare lattice).

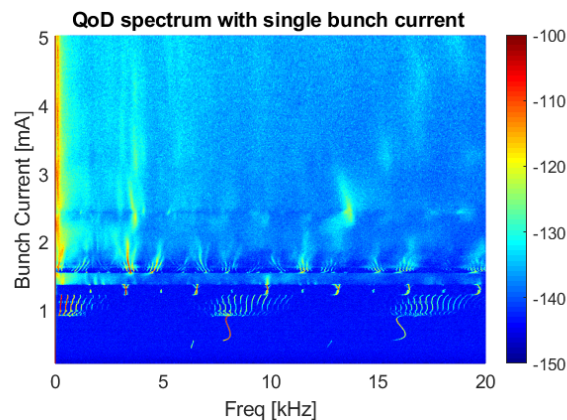


Figure 6: QoD signal spectra at different single bunch current. $V_{rf} = 1.5\text{MV}$, all ID gaps open (bare lattice).

Table 1: Threshold Currents to See the Microbunching Sidebands

ID gaps	V_{rf} [MV]	I_{th} [mA]
All closed	3	1.2
3DW closed	3	1.27
All open (bare)	3	0.3
All open (bare)	1.5	0.46

Power Measurement

In addition to the single bunch spectra discussed above, QoD measurements were carried out during normal operations and other studies. The carrier signal level was measured.

Figure 7 gives the QoD signal level measurement with 0.45mA single bunch stored in the ring, and RF voltage was varied so that bunch lengths changed. When the bunch lengths were shorter (at higher RF voltage), the QoD signal was higher. As RF voltage decreased below 2MV, the QoD measured signal was about 1uA (-107dBm) which was approaching the spectrum analyzer noise floor. Single bunch current decreased to 0.41mA at lower RF voltage.

Figure 8 is the QoD measured signal during 450mA studies, where two fill/scraping were available. Beam was filled to 450mA in 1200 bunches, with per bunch current of 0.375mA. The second fill was with 1000 bunches and a bunch current of 0.45mA. In both cases, beam was scrape down from high current and QoD signal was recorded during the period.

As seen in Fig. 8, both fills have more or less same QoD signal when total beam current was below 100mA, as beam current increased, the 1000-bunch fill has higher signal. At the same 450mA, the QoD signal increased from 7.17mV with 1200 bunches to 8.16mV with 1000 bunches.

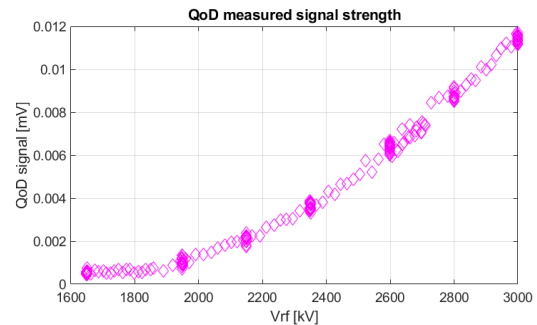


Figure 7: Vary RF cavity voltage to see the QoD signal, 0.45mA single bunch was stored in the ring.

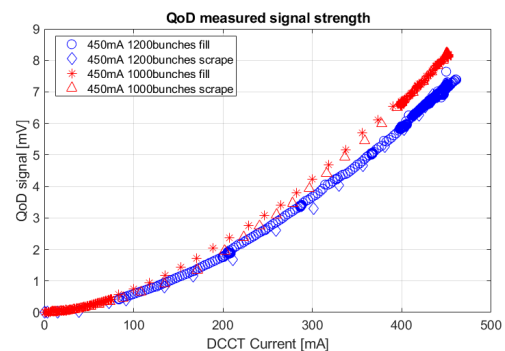


Figure 8: Two different fills to 450mA and scrape down. RF voltage was at 2.6MV for both fills.

Discussion

The cutoff frequency of dipole vacuum chambers is limited by its height. Synchrotron radiations can only propagate with wavelengths shorter than the cutoff frequency. For nominal dipole chamber, the slot height of 10mm gives a cutoff wavelength of 0.4mm (cutoff frequency of 750 GHz). While for IR beamline dipole chamber, the height was increased to 76mm, the cutoff wavelength is 8.4mm (36 GHz). The cutoff wavelength of vacuum chamber is $\lambda_0 = 2h \cdot (h/\rho)^{1/2}$, where h is chamber height and ρ is the dipole radius (25m for NSLS-II dipoles). Microwave signal from beam wakefield may be present in both beamlines, and propagates to the detector together with synchrotron radiations.

Schottky diode setups have been tested at both beamlines. There were microwave signals measured with diodes sensitive to 30-110GHz signals [11]. Different from QoD detector which can detect both high frequency synchrotron radiations, as well as microwave signals. The diodes sensitive to <100GHz signal will only see microwave signal at the visible diagnostic beamline. We hope to report in the future the comparison of QoD and Schottky diodes results. Array of detectors, like the setup at Diamond Light Source [12], can be useful to distinguish the microwave and synchrotron radiation signals.

Interferometer can be setup at the IR beamline to measure the detected signal spectra.

SUMMARY

A QoD detector has been used at NSLS-II to measure 100GHz to 1THz signals at the IR beamline and visible diagnostic beamline.

With normal operational lattices and momentum compaction factor, clear microbunching instabilities were observed at higher single bunch current. The threshold currents depend on the bunch lengths, which are affected by the ID gaps and RF voltages. With all ID gaps open, the threshold current is below 0.5mA which is the per bunch current at 500mA (filled in 1000 bunches). The threshold currents are above 1mA when the damping wigglers are closed.

REFERENCES

- [1] G. L. Carr, S. L. Kramer, J. B. Murphy, et. al., "Observation of coherent synchrotron radiation from the NSLS VUV ring", Nucl. Instrum. Meth. Phys. Res., A 463, 387 (2001)
- [2] M. Abo-Bakr, J. Feikes, K. Holldack, et. al., "Steady-State Far-Infrared Coherent Synchrotron Radiation detected at BESSY II", Phy. Rev. Lett. 88, 254801 (2002)
- [3] J. M. Byrd, W. P. Leemans, A. Loftsdottir, et. al., "Observation of Broadband Self-Amplified Spontaneous Coherent Terahertz Synchrotron Radiation in a Storage Ring", Phy. Rev. Lett. 89, 224801 (2002)
- [4] R. Bartolini, G. Cinque, G. Rehm, C. A. Thomas, and I. P. S. Martin, "CSR and THz Emission Measurements at the Diamond Light Source", in *Proc. IPAC'11*, San Sebastian, Spain, Sep. 2011, paper THPC068, pp. 3050-3052.

- [5] G. Rehm, R. Bartolini, V. Karataev, I. P. S. Martin, and A. F. D. Morgan, "Ultra-Fast mm-Wave Detectors for Observation of Microbunching Instabilities in the Diamond Storage Ring", in *Proc. DIPAC'09*, Basel, Switzerland, May 2009, paper TUPD32, pp. 369-371.
- [6] V. Judin *et al.*, "Spectral and Temporal Observations of CSR at ANKA", in *Proc. IPAC'12*, New Orleans, LA, USA, May 2012, paper TUPPP010, pp. 1623-1625.
- [7] P. Kuske, "Investigation of the Temporal Structure of CSR-Bursts at BESSY II", in *Proc. of PAC'2009*.
- [8] C. Evain *et al.*, "Microbunching Instability Studies at SOLEIL", in *Proc. IPAC'11*, San Sebastian, Spain, Sep. 2011, paper MOPS048, pp. 709-711.
- [9] W. X. Cheng *et al.*, "Experimental Study of Single Bunch Instabilities at NSLS-II Storage Ring", in *Proc. IPAC'16*, Busan, Korea, May 2016, pp. 1738-1740. doi:10.18429/JACoW-IPAC2016-TUP0R033
- [10] <https://acst.de/products/quasi-optical-detectors/>
- [11] S. Kramer, private communication
- [12] A. Finn, P. Karataev, and G. Rehm, "A Multi-band Single Shot Spectrometer for Observation of mm-Wave Bursts at Diamond Light Source", in *Proc. IPAC'15*, Richmond, VA, USA, May 2015, pp. 1126-1128. doi:10.18429/JACoW-IPAC2015-MOPTY080